J Mater Sci (2016) 51:1680–1691
DOI 10.1007/s10853-015-9452-8

HTC 2015

Thermophysical properties of some Ni-based superalloys in the liquid state relevant for solidification processing

S. Amore[1] · F. Valenza[1] · D. Giuranno[1] · R. Novakovic[1] · G. Dalla Fontana[2] · L. Battezzati[2] · E. Ricci[1]

Received: 6 July 2015 / Accepted: 21 September 2015 / Published online: 28 September 2015

Abstract The thermophysical properties, e.g., melting range, specific heat, solid fraction, density, and surface tension of four industrial Ni-based alloys, namely MC-2, CMSX-10, TMS-75, and LEK-94, have been determined within the ground-based experiments program of the ESA MAP ThermoProp project. The tests were performed under reducing atmosphere in order to lower the oxygen contamination. The results obtained have been compared with the corresponding data of Ni-based alloys available in literature. The new experimental data have been analyzed as a function of both temperature and alloy composition and interpreted by means of different thermodynamic models.

Introduction

The production of metallic alloys is characterized by an increasing level of sophistication brought about by the progress in the modeling of liquid metal processing and of solidification for the prediction of microstructures: models describing fluid and heat flow are combined with thermodynamic models of phase stability and selection.

In order to take full advantage of these technological and scientific developments, accurate values of the thermophysical properties are needed as input for the models. However, the full availability of such kind of values currently lacks due to the high chemical reactivity of Ni-based superalloy melts in contact with surrounding atmospheres and/or containers. The thermophysical properties of several Ni-based superalloys [1] have been determined within the ground-based experiments program of the ESA MAP ThermoProp project. The project is concerned with the measurement of the thermophysical properties of industrial alloys in the liquid phase and combines long and short duration microgravity measurements with ground-based experiments [2, 3].

In this work, the new experimental datasets for the solidus and liquidus temperatures, specific heat, heat of fusion, surface tension, and density of four industrial Ni-based superalloys are presented with special attention to the effects of Al content, ranging between 11 and 14 at %, on the above-mentioned properties. High-temperature calorimetry was employed to measure the thermal properties of the alloys selected [4]. The values of melting range were also used as reference data in the surface tension and density measurements, which were performed by the large drop method [5] in the temperature range 1653–1753 K, under a reducing atmosphere. In addition, the surface tension and density results were analyzed by different thermodynamic models (e.g., ideal solution, regular solution, and compound-forming model) [5, 6] in order to interpret the experimental data obtained as a function of both temperature and alloy composition.

Materials and methods

Materials

Four commercial Ni-based superalloys have been investigated. Their nominal compositions together with the

✉ E. Ricci
e.ricci@ge.ieni.cnr.it

[1] Consiglio Nazionale delle Ricerche, Istituto per l'Energetica e le Interfasi (CNR-IENI), Via de Marini, 6, 16149 Genoa, Italy

[2] Dipartimento di Chimica, Università di Torino, Via Pietro Giuria 7, 10125 Turin, Italy

compositions resulting from the EDX analyses are shown in Table 1.

All the alloys as received have been analyzed by Energy-dispersive X-ray spectroscopy (EDX) analysis, to check the real composition. Micrographically polished surfaces of the superalloys were observed by scanning electron microscopy (SEM, model: LEO 1450 VP) and analyzed by electron microprobe (EDX) (Oxford Instruments, 7353 model with Oxford-INCA software v. 4.07, type of detector: Li-doped Si). EDX analyses were performed on at least five areas for each sample to determine the composition. The following parameters were used: working distance of 15 mm, live time was 40 s, acceleration voltage of 20 kV, current of 1.5 pA, and standard element was Co. By using these parameters, the detection limit is 0.1 wt %, while the precision is 1 wt %. The EDX composition of each superalloy, reported in Table 1, is close to the corresponding nominal one, except in the cases of the TMS-75 and LEK-94 alloys. Indeed, Al content detected in the TMS-75 is lower than the corresponding nominal content (Table 1) and it is comparable to its Co content. Similarly, in the LEK-94, the Al content detected is higher than the nominal one. Such discrepancies can be explained by the inhomogeneity of the alloys, probably caused by the processing routes.

Leica Stereoscan 420 scanning electron microscope was used to examine the microstructures of the samples after an acid attack (HCl, H_2SO_4, HNO_3). The presence of cuboids (γ') immersed in the γ matrix was detected in some samples, as well as some precipitates, probably associated to carbides, indicating a typical microstructure of Ni-based superalloys [7].

In the following, the indicated atomic percentage of Al corresponds to the composition analyzed by EDX.

Experimental apparatuses and procedures

Measurements of thermal properties have been performed by high-temperature differential scanning calorimeter (HTDSC Setaram) under flowing He filtered with metal sponge to remove residual oxygen and water vapor. The cell is made of alumina and the sample is contained in an alumina pan with some alumina powder to prevent it from sticking to the crucible walls. The cell was evacuated and purged several times before measuring. Various experiments were performed with heating rates of 2, 5, and 10 K min^{-1}. The frequency of sampling of the data points was one point every 1–3 s, according to the heating or cooling rate for a total of 4800 points per file. Calibration of the apparatus has been performed by measuring the temperature and heat of fusion of samples of pure metals (Al, Ag, Au, Fe, Cu, Ni) on both heating and cooling. The specific heat was also calibrated with samples of sapphire and pure metals either in wide temperature ranges by continuous heating or at steps of a few tens of degrees (enthalpy method) [8].

To measure the density and surface tension, a variant of the large drop method called pinned drop method was applied [9]. In this case, the solid support is a special circular crucible with sharp edges. The design of the edges of the crucible blocks the triple line at an apparent contact angle that is much higher than the real one [5]. A further advantage of the pinned drop method is that the axi-symmetry of the drop can be imposed. The experiments were carried out using an apparatus built expressly for this purpose.

The furnace could reach a maximum temperature of 1873 K and is made of two concentric, horizontal, alumina tubes; between the two tubes, a constant flow of argon

Table 1 Nominal (Nom) composition (in at %) of the Ni-based superalloys investigated

Name	Alloy composition at %										
	Al	Ti	Cr	Co	Mo	Ta	W	Re	Hf	Nb	Ni
MC-2											
Nom	11.2	1.9	9.3	5.2	1.3	2.0	2.6	–	–	–	Bal.
EDX	*11.3*	*1.7*	*9.6*	*5.2*	*1.4*	*2.3*	*3.3*				
TMS-75											
Nom	13.7	–	3.6	12.6	1.3	2.1	2.2	1.7	0.03	–	Bal.
EDX	*12.9*	–	*3.2*	*12.4*	*1.0*	*2.1*	*2.4*	*1.5*			
CMSX-10											
Nom	13.2	0.3	2.4	3.18	0.26	2.76	1.7	2.01	0.01	0.06	Bal.
EDX	*13.5*	*0.0*	*2.6*	*5.7*	*0.0*	*2.9*	*2.2*	*1.9*	*0.0*	*0.0*	
LEK-94											
Nom	13.8	1.2	6.7	7.3	1.2	0.7	1.0	0.8	0.03		Bal.
EDX	*14.9*	*1.1*	*6.8*	*7.5*	*1.4*	*0.9*	*1.5*	*1.1*			

The results of EDX analysis are also reported

guarantees that, even in the temperature range up to 1873 K, oxygen does not diffuse inside the experimental chamber. Temperature is read by S-type thermocouple, placed just below the test specimen, which was calibrated against the melting points of Au, Cu, Ni, and Fe slabs placed in the same place of the test specimen. The precision of the temperature reading can be estimated in ±5 K. Tests could be performed in ultra high vacuum (10^{-1} Pa at 1273 K), thanks to a turbomolecular pump or under controlled atmospheres. The oxygen partial pressure of the working atmosphere is continuously monitored by solid-state oxygen sensors at the chamber inlet and outlet.

The superalloy samples of about 3 g were carefully prepared (mechanical and ultrasonic cleaning) and placed in a sapphire crucible ($r_i = 5.5$ mm). For various applications involving the melting of nickel and/or its alloys, sapphire (Al_2O_3 single crystal) is the best choice in comparison with polycrystalline alumina ceramics because of its low chemical reactivity. All the measurements have been carried out under a constant flow of Ar-5 % H_2 mixture (flow rate 3 l/h). In addition, a Zr-getter, placed close to the sample, was used to further reduce the oxygen content. Therefore, for the experimental temperature range, the chemical equilibrium between Zr and oxygen ensured the oxygen partial pressure close to sample was in the range $P_{O2} = 10^{-21} \div 10^{-18}$ Pa. Once equilibrium conditions have been attained, the sample was introduced at the center of the test chamber with the magnetic push rod.

At each temperature, the sample was allowed to equilibrate for a time ranging from 10 to 20 min. The profile of the liquid drop was acquired using a CCD camera for a time $t = (10–15)$ min. The acquisition frequency can be up to ten points per second with an accuracy up to 0.1 %. The surface tension was calculated by using a nonlinear regression method developed by Maze and Burnet [10]. The images were processed with a dedicated acquisition software in a LABView® environment which allows the elaboration of surface tension and other drop parameters in real time. The density values were obtained from the ratio of the drop weight and the measured volume at each temperature during the pinned drop experiments. In order to ensure accurate results, the calibration of experimental apparatus using a sample of pure gold has been performed.

All the experimental values obtained are results of different measurement runs. Considering the experimental uncertainties, the total error in the surface tension and density values is estimated to be about 3 %. After each experiment, the samples have been further analyzed by SEM-EDX in order to check the surface conditions of the solidified drop and neither changes in sample compositions nor mass losses were observed. The oxygen content detected by EDX at the top surface was lower than 5 at %.

Results and discussion

Melting range and specific heat

An example of calorimetric results is reported in Fig. 1 for the TMS-75 superalloy. In all curves, a broad peak occurring in the solid state (barely visible in this plot because of the scaling, but clearer in Fig. 2) is caused by the dissolution of the γ' precipitates. The solvus is taken as the end temperature of the broad peak. The main endothermal peak is due to melting of the sample. The solidus temperature is taken when a deflection from the baseline is detected. The melting peaks are composed of two contributions in all cases showing the effect of the coexistence of the main solid solution with residual phases (e.g., carbides). The composite shape of the exothermal peak obtained on cooling for solidification is due to dendrite formation on undercooling followed by freezing of the remaining liquid. The liquidus temperature was obtained by extrapolation to 0 K min^{-1} of the apparent T liquidus at three different speed (2, 5, and 10 K min^{-1}, inset in Fig. 1).

The integral of the melting/solidification signals provides the enthalpy of fusion with a scatter of values of the order of ±10 %. This is taken as an estimate of the error in the specific heat data as well as an example of which is reported in Fig. 2. Specific heat data obtained with the enthalpy method at selected temperatures are shown as points. They confirm the continuous curve within the data

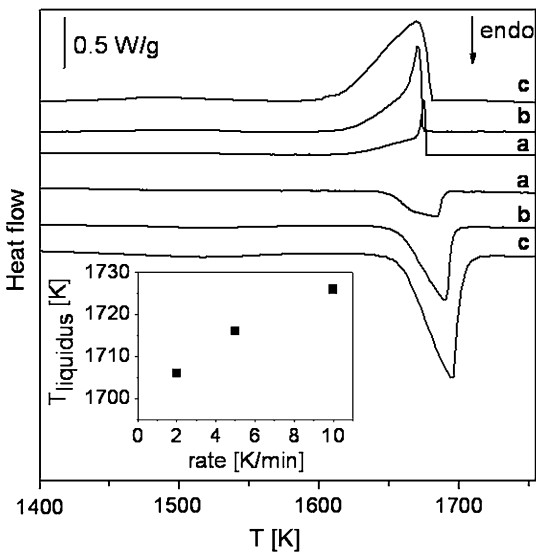

Fig. 1 Thermograms obtained on heating (*lower curves*) and cooling (*upper curves*) of the TMS-75 superalloy: **a** 2 K/min, **b** 5 K/min, **c** 10 K/min. The curves have been shifted along the *y*-axis for clarity. Solvus, solidus, liquidus, and solidification temperatures are collected from these traces and reported in Table 2. The inset shows the extrapolation of the liquidus temperature to 0 K/min

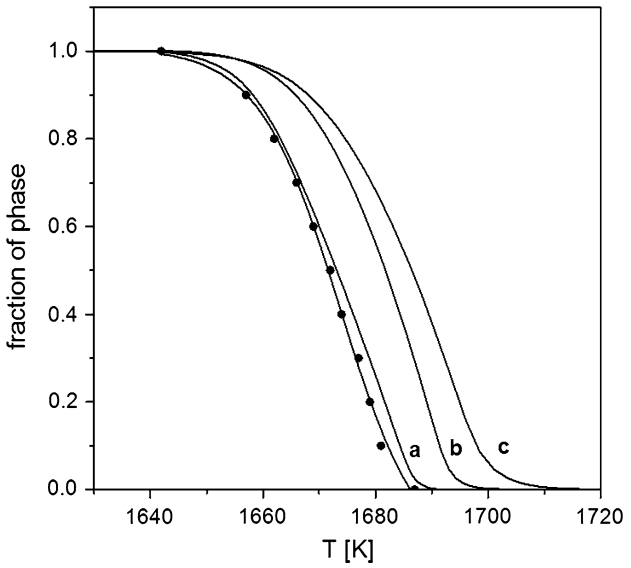

Fig. 2 Solid fraction of the TMS-75 superalloy obtained from HTDSC (**a** 2 K/min, **b** 5 K/min, **c** 10 K/min) and from their extrapolation to nil cooling rate

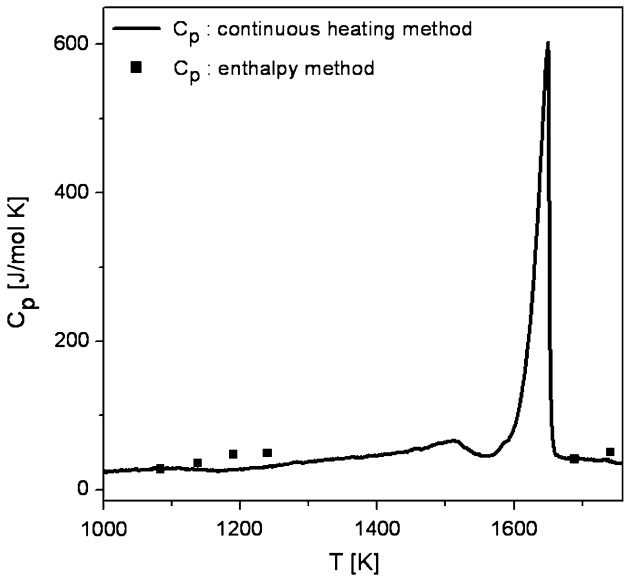

Fig. 3 The specific heat of the MC-2 superalloy obtained with the continuous heating and enthalpy methods. The dissolution and melting peaks provide an apparent increase in specific heat

scatter. The values are close to the ideal specific heat provided by the Neumann–Kopp rule for all four alloys analyzed in this work, as shown in Table 2.

Solid fraction

The solid fraction as a function of temperature is an important parameter in solidification modeling. The experimental cooling curves obtained by HTDSC detect the occurrence of solidification on undercooling which makes these measurements unsuitable for the determination of the equilibrium solid fraction. Therefore, data for this quantity are derived by integrating the melting peak on heating as a function of temperature (Fig. 3). Sigmoidal curves are obtained and displaced on the temperature axis as a function of heating rate. In order to cancel this effect, an extrapolation procedure has been devised. For every solid fraction value, the corresponding temperatures obtained at each rate have been linearly fitted and extrapolated to zero rate obtaining the dotted curve of Fig. 3. It should be noted that the solid fraction obtained by integrating the solidification peak at a given rate is representative of the actual alloy behavior when these rates are employed in processing.

In Table 2, a summary of the relevant temperatures,enthalpies of phase transformation on heating and cooling, and specific heat capacity with the corresponding temperature range of the superalloys investigated in this work is given.

Enthalpies of melting for a number of superalloys are collected in Fig. 4 as a function of Al content. It shows

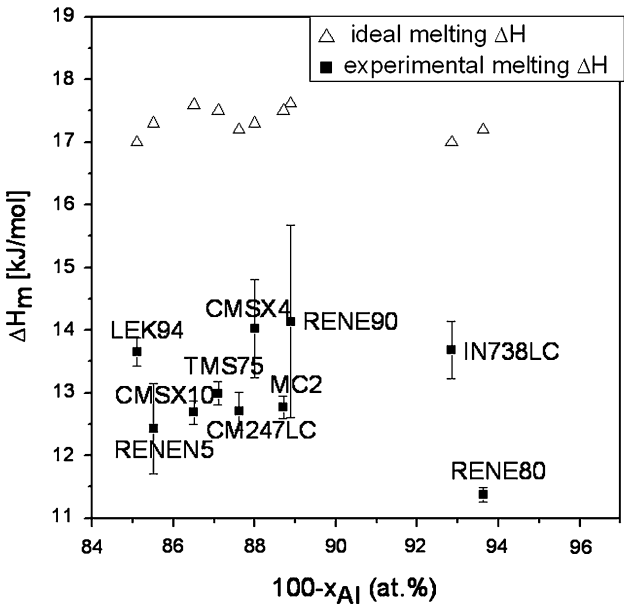

Fig. 4 Experimental and ideal values of the enthalpy of melting of some superalloys as a function of Al content

clearly that the enthalpies are far below the ideal melting enthalpy computed with Richard's rule [11]. This is a straightforward indication that the excess free energy of mixing in the liquid state is less (i.e., more negative) than that in the solid state and, therefore, that the liquid has a degree of order at short range as earlier discussed for the binary Al–Ni system [4] and proven further by surface tension experiments and calculation reported below.

Density

The density of MC-2, TMS-75, CMSX-10, and LEK-94 Ni-based superalloys has been measured in the temperature range (T_{min}–T_{max}). The density values (ρ_L) at the liquidus temperature (T_L) (Table 2), the corresponding temperature coefficients (dρ/dT), together with the actual Al content (x_{Al}) of the four Ni-based superalloys investigated, are shown in Table 3. In addition, the experimental values of the surface tension at the liquidus temperature (σ_L) and the surface tension coefficients (dσ/dT), that will be described later on, are displayed.

In Fig. 5, the experimental density values of the four Ni-based superalloys investigated are shown as a function of temperature. For all superalloys, the density increases with a decrease in Al content and its temperature dependence is described by linear relationships (Table 3). The standard deviation associated to each density value, shown in Fig. 5, is less than 1 %. However, the total uncertainty of the measure can be estimated to be less than 5 %.

As already discussed in [12], the measured density values of the Ni-based superalloys are consistently higher than those calculated by the ideal mixture approximation. This behavior is confirmed by the present results as shown in Fig. 6, where the density experimental data obtained in the present work are compared with two isotherms, calculated for 1773 K with the ideal solution model and taking into account the contribution of the excess volume [13, 14].

Comparable values varying between 5 and 6 % were reported for several commercial Ni-based superalloys, included CMSX-10 and TMS-75 [15, 16]. These findings can be justified by the mixing property data of liquid Al–Ni alloys [5, 17, 18]. Indeed, the thermodynamic data of the Al–Ni system [18] indicate a pronounced negative deviation from the Raoult law in agreement with the results on the enthalpy of melting of the Ni-based alloys investigated. The negative enthalpy of mixing is due to preferential bonding between Al and Ni atoms and corresponds to a

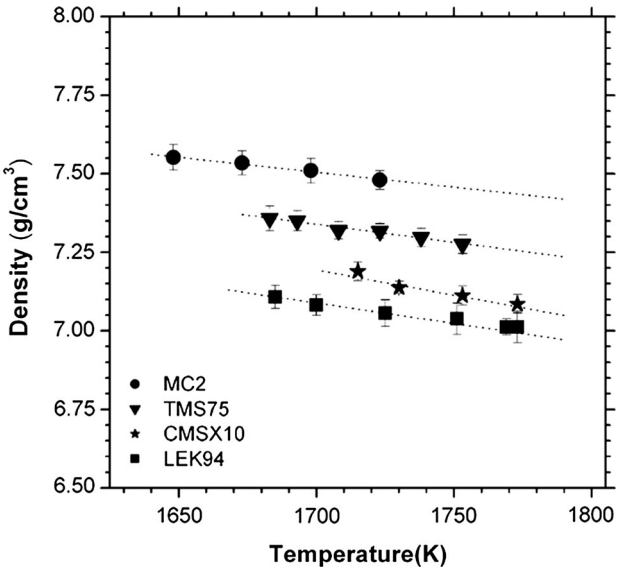

Fig. 5 Density as a function of temperature of Ni-based superalloys: (*filled circle*) MC-2 (*filled inverted triangle*) TMS-75; (*filled star*) CMSX-10; (*filled square*) LEK-94. *Dotted lines* linear fit of measured data

Table 2 Relevant temperatures (T_x); enthalpies of phase transformation on heating and cooling (ΔH_x); specific heat capacity (C_p) with the corresponding temperature range, of the four superalloys investigated in this work

Alloy	T_{solvus} (K)	$T_{solidus}$ (K)	$T_{app.\ liquidus}$ (K)	$T_{liquidus}$ (K)	$T_{nucleation}$ (K)	ΔH_m (J/g)	ΔH_s (J/g)	Cp (J/g K)	T Range for liquid Cp (K)
MC-2	1550 ± 2	1562 ± 2	1674 ± 15	1651 ± 6	1645 ± 3	211 ± 3	211 ± 3	0.7	1670–1730
TMS-75	1588 ± 3	1633 ± 2	1715 ± 10	1702 ± 2	1683 ± 5	209 ± 3	203 ± 3	0.6	1675–1710
CMSX-10	1635 ± 6	1647 ± 1	1722 ± 15	1702 ± 4	1689 ± 2	210 ± 2	209 ± 4	0.7	1690–1730
LEK-94	1568 ± 2	1592 ± 8	1683 ± 11	1668 ± 2	1668 ± 2	199 ± 4	191 ± 4	0.75	1650–1750

Table 3 Density (ρ_L), density coefficient (dρ/dT), surface tension (σ_L), and surface tension coefficient (dσ/dT) of the four Ni-based superalloys investigated

Alloy	x_{Al} (at %)	T_L (K)	T_{min}–T_{max} (K)	ρ_L (g cm^{-3})	dρ/dT (g cm^{-3} K^{-1})	σ_L (mN m^{-1})	dσ/dT (mN m^{-1} K^{-1})
MC-2	11.3	1651	1653–1723	7.56 ± 0.07	−0.00130	1838 ± 45	−0.51 ± 0.04
TMS-75	12.9	1702	1683–1753	7.37 ± 0.07	−0.00115	1805 ± 44	−0.49 ± 0.04
CMSX-10	13.5	1702	1715–1773	7.19 ± 0.03	−0.00160	1758 ± 25	−0.47 ± 0.04
LEK-94	14.9	1668	1685–1773	7.13 ± 0.06	−0.00095	1718 ± 40	−0.52 ± 0.04

The Al content (x_{Al}), the liquidus temperature (T_L), and the experimental temperature range (T_{min}–T_{max}) for each alloy are also reported

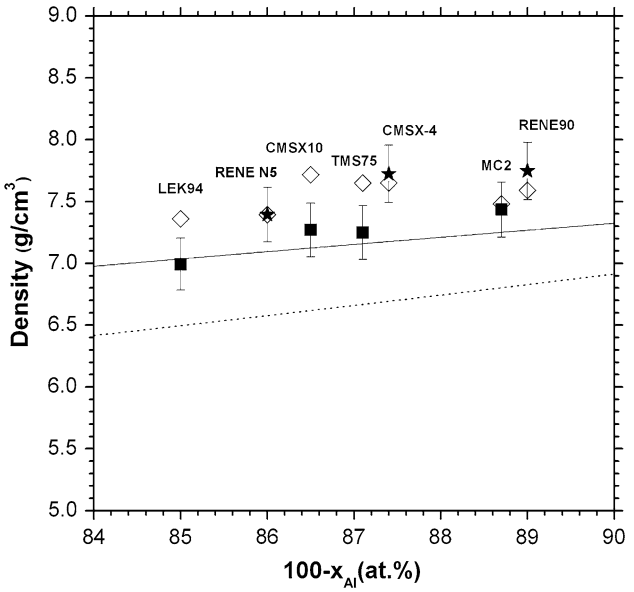

Fig. 6 Comparison between the density experimental data of Ni-based superalloys and the calculated density isotherms. *Dotted line* ideal solution model; *full line* considering the excess volume [13]. Experimental and theoretical data are calculated at $T = 1773$ K and reported as a function of Ni content in the alloy. (*filled square*) present work; (*filled star*) literature data from [12] and [22]; (*diamond*) density calculated as linear combination over all the elements

decrease in the molar volume with respect to those of an ideal mixture [11].

Mukai et al. [15, 19] have used two experimental methods to measure the density of liquid Ni and of a series of Ni-based alloys, both binary and complex multicomponent systems of industrial interests, aiming at assessing a general prediction model for the densities of liquid Ni-based alloys [15].

In Fig. 7, the comparison between the experimental density data obtained in the present work and those collected from the literature is shown. Both experimental and calculated data are available for CMSX-10 and TMS-75 superalloys [16, 20]; while for MC-2 and LEK-94 superalloys, due to the lack of available experimental data, only values estimated by applying the Mukai model [15] can be considered.

The density of TMS-75 obtained in the present work is slightly lower (about 5 %) than the two datasets measured by Li et al. by means of two different methods [16]. In addition, the measured data reported are in good agreement with the corresponding predicted values [15]. The experimental literature data for CMSX-10 [16, 20] and the predicted values are higher than the new experimental data and exhibit a maximum difference of about 11 %. Although this difference could be attributed to the different techniques adopted and to a slight variation in the alloy compositions, further investigations are needed.

The experimental density results obtained for both MC-2 and LEK-94 compared with the predicted values by the Mukai model [15], exhibit difference < 1.5 and 3 %, respectively, within the total uncertainty of the measurements.

It is worth to be noted that the differences between the present experimental data and those predicted become larger from the alloy melting point to the end of the temperature interval of measurements due to different density temperature coefficients with respect to the calculated curves [15, 21].

In addition, the density behavior of MC-2 and LEK-94 as a function of temperature seems to further confirm the effect of Al content on this property (Table 1).

Surface tension

The surface tension of the Ni-based superalloys has been measured in the same temperature range (Table 3). Each measured value shows a standard deviation less than 1 % as reported in Fig. 8. The new surface tension data as a function of temperature together with the experimental data of the Ni-based superalloys previously measured under the same experimental conditions [12, 22] are shown in Fig. 8.

The surface tension of the superalloys investigated obeys a linear law over the measured temperature ranges. The linear fit obtained by the least square method provides the values of σ_L and $d\sigma/dT$ with the error limits lower than 2 and 8 %, respectively. The values of their temperature coefficients expressed by the average value are in agreement with each other and can be given as 0.49 ± 0.04 (mN m^{-1} K^{-1}).

A dependence on the actual Al content in the alloy (Table 1) can be revealed: the surface tension decreases with increasing the Al content in the alloy, mainly because of the lower surface tension of Al with respect to the other alloy components.

The surface tension data of the superalloys investigated mainly are consistent with each other with respect to the Al content in the alloys. To our knowledge, the surface tension data of MC-2, TMS 75, and LEK-94 liquid superalloys are not available in the literature, while in the case of CMSX-10, the data were reported by Li et al. [16]. However, these authors observed an increase of the surface tension with the increasing temperature, typical behavior of liquid alloy samples with high soluble oxygen content, and for this reason, their data were not taken into account neither in the comparison nor in the analysis and interpretation of new experimental data.

In order to analyze the effects of highly reactive alloy components, such as Al, Ta, Ti, and Re (Table 1) on the surface tension of investigated superalloys, the new experimental data were compared with literature data of the

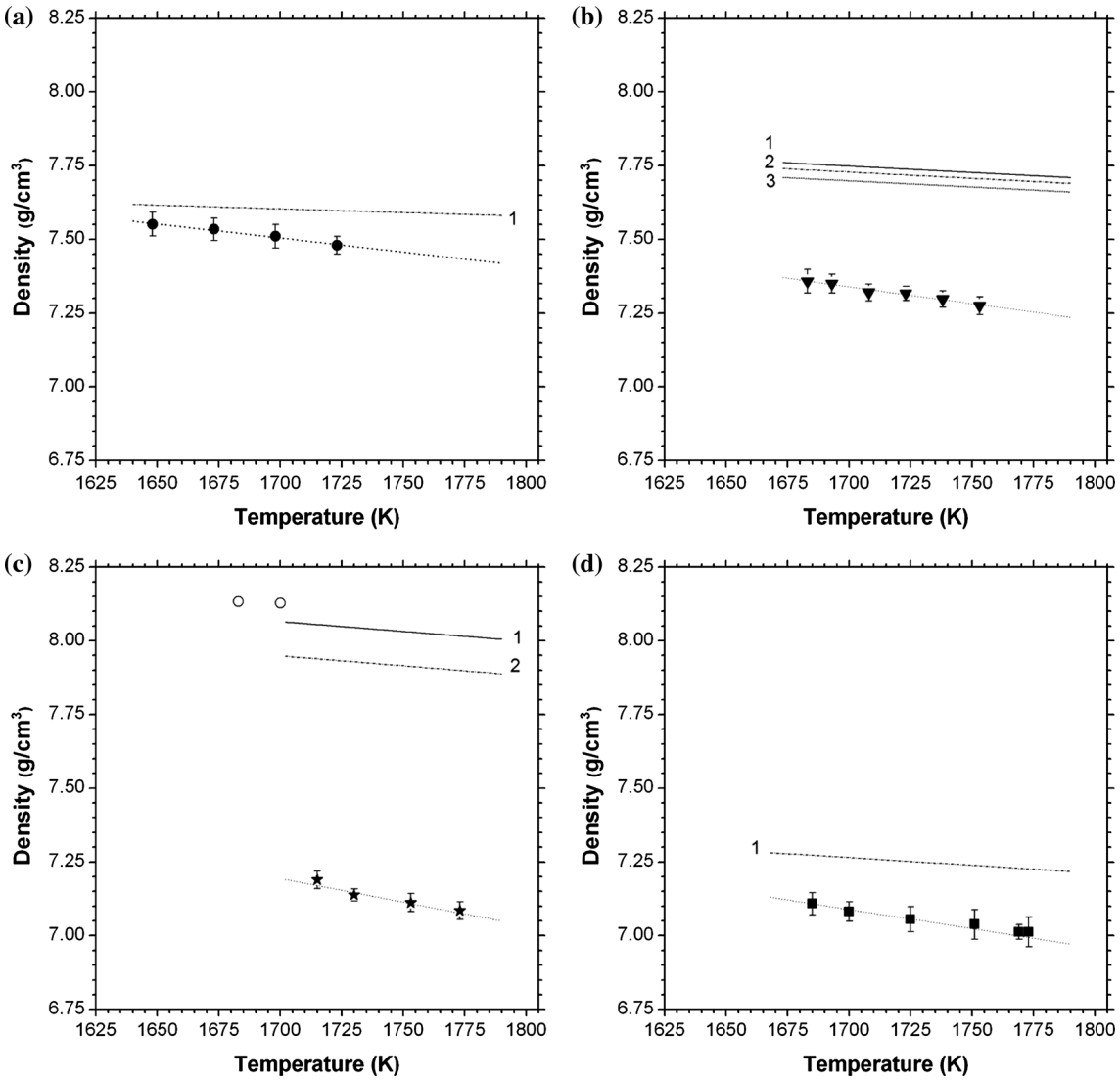

Fig. 7 Density as a function of temperature of Ni-based superalloys: **a** (*filled circle*) MC-2; **b** (*filled inverted triangle*) TMS-75; **c** (*filled star*) CMSX-10; **d** (*filled square*) LEK-94. *Dotted lines* are the linear fits of the measured data. The data obtained in the present work are compared with the predicted data: **a** *line 1* from [15]; **b** *line 2* from [15]; **c** *line 2* from [15]; **d** *line 1* from [15]; and with literature measured data: **b** *lines 1* and *3* from [16]; **c** *line 1* from [16] and *circle* from [20]

CMSX-4 [22], RENE-N5 [12], and RENE-90 [12] having similar compositions. Among the datasets shown in Fig. 8, the surface tension data of CMSX-4 [22] result lower than expected with respect to the Al content in the entire temperature range of measure. However, the surface tension of CMSX-4 as a function of temperature has been widely discussed in the literature [16, 21, 23, 24], showing that its surface tension values exhibit a large scatter. That reveals the difficulty of obtaining reproducible results which seems to be particularly influenced by the combined effects of highly reactive elements, such as Ti and Re [12, 16] and gaseous surfactants [9]. Furthermore, differences in the chemical compositions of CMSX 4 have been reported which may also have influence on the measured data [22, 24].

In fact, as discussed in our previous work [12], the presence of both metals having a surface tension higher (Ti, Cr, Mo, W) than that of Ni and refractory metals (Re, Hf) as minor components could induce higher surface tension. On the other hand, most of these components are strongly reactive with surface active elements, mainly oxygen or/and sulfur, which can drastically reduce the surface tension and thus affect the reliability of the data [5].

The new surface tension data were further analyzed in the framework of thermodynamic models. Generally, when dealing with properties of multicomponent alloy systems, it is possible to estimate a property value analyzing a key binary and/or ternary subsystem formed by the major components of a complex system of interest and taking into account the effects of its minority components on that

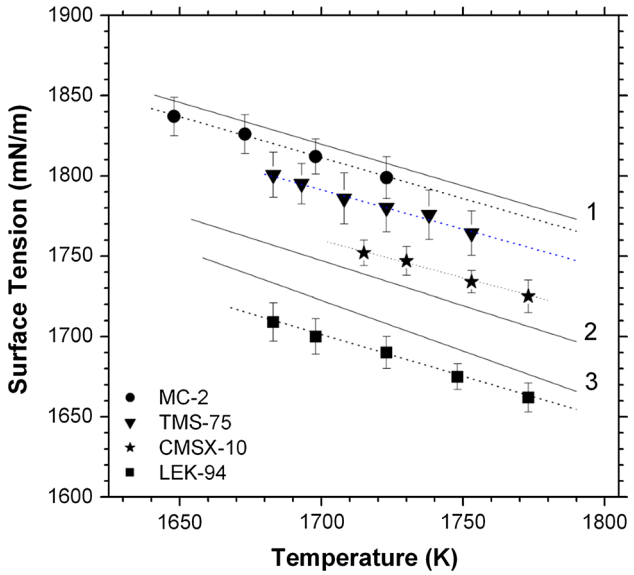

Fig. 8 Surface tension as a function of temperature of Ni-based superalloys: (*filled circle*) MC-2; (*filled star*) CMSX-10; (*filled inverted triangle*) TMS-75; (*filled square*) LEK-94. *Dotted lines* linear fit of measured data. The data obtained in the present work are compared with the literature data: *1* RENE-90 [12]; *2* CMSX-4 [22]; RENE-N5 [12]

property. In the case of Ni-based superalloys here investigated, Ni, Al, and Cr or Co are the major alloying elements (Table 1), and hence, the new surface tension values of four Ni-based superalloys were compared to the model-based predictions related to the Al–Ni binary system as well as to the Al–Co–Ni or Al–Cr–Ni ternary systems [5, 12, 17]. The surface tension of binary subsystems has been calculated by using the ideal (perfect) solution model, the quasi-chemical approximation (QCA) for the regular solutions, and the compound formation model (CFM), and subsequently extended to main ternary subsystems of Ni-based superalloys investigated. The main hypothesis of the aforementioned models is that the surface is considered as an additional thermodynamic phase, in equilibrium with the bulk. In the framework of the CFM, the atoms of pure metal components are in equilibrium with a group of atoms or short-range ordered elements having the stoichiometry of an energetically favored intermetallic compound present in the solid state. The absence of clusters in the melt reduces the model to the QCA for regular solutions. It is important to mention that the QCA results are very close to those obtained by the Butler equation [5, 25]. Mathematical formalisms of thermodynamic models applied in the present work to calculate the surface tension of liquid binary alloys have been described in detail in our previous papers [5, 12, 17, 25]. For the sake of clarity, we recalled a few basic equations (Eqs. 1–3) used to predict the surface tension isotherms.

The thermodynamic data and the optimized datasets of the excess Gibbs free energy of mixing of liquid Al–Ni [18], Al–Cr–Ni [26] and Al–Co–Ni [27], the densities and molar volumes of pure components [11], as well as the surface tension reference data of Al [28], Ni [29], Cr [30], and Co [31] were taken as input data for the calculations of the surface tension isotherms and iso-surface tension lines.

The surface tension of liquid Al–Ni alloys has been investigated by the ideal or perfect solution model, by the QCA for the regular solution [32, 33], and by the CFM [5, 34], given by Eqs. (1–3), as follows

$$\sigma = -\frac{k_B T}{\alpha}\ln\left[C\exp\left(-\left(\frac{\sigma_A \alpha}{k_B T}\right)\right) + (1-C)\exp\left(-\left(\frac{\sigma_B \alpha}{k_B T}\right)\right)\right] \tag{1}$$

$$\sigma = \sigma_A + \frac{k_B T(2-pZ)}{2\alpha}\ln\frac{C^s}{C} + \frac{Zk_B T}{2\alpha}\left[p\ln\frac{(\beta^s - 1 + 2C^s)(1+\beta)}{(\beta^s - 1 + 2C)(1+\beta^s)} - q\ln\frac{(\beta - 1 + 2C)}{(1+\beta)C}\right] \tag{2a}$$

$$\sigma = \sigma_B + \frac{k_B T(2-pZ)}{2\alpha}\ln\frac{(1-C^s)}{(1-C)} + \frac{Zk_B T}{2\alpha}\left[p\ln\frac{(\beta^s + 1 - 2C^s)(1+\beta)}{(\beta^s + 1 - 2C)(1+\beta^s)} - q\ln\frac{(\beta + 1 - 2C)}{(1+\beta)(1-C)}\right] \tag{2b}$$

$$\sigma = \sigma_A + \frac{k_B T}{\alpha}\ln\frac{C^s}{C} + \frac{k_B T}{\alpha}\ln\frac{\gamma_A^s}{\gamma_A} \tag{3a}$$

$$\sigma = \sigma_B + \frac{k_B T}{\alpha}\ln\frac{(1-C^s)}{(1-C)} + \frac{k_B T}{\alpha}\ln\frac{\gamma_B^s}{\gamma_B}. \tag{3b}$$

In Eqs. (1–3), σ is the surface tension, σ_A and σ_B are the surface tensions of alloy components A and B, C and $1 - C$ are their mole fractions, α is the mean value for atomic area of the components calculated from surface areas of each species, k_B is the Boltzmann constant, and T is temperature. In Eq. (2), the auxiliary variable β contains implicitly the order energy term, W [32]. β^s is the function obtained from β by substituting the bulk concentration C by the surface concentration C^s. p and q are the surface coordination fractions and Z is the coordination number [5, 32]. In Eq. (3), γ^A, γ^B, γ_A^S, and γ_B^S are the activities of alloy components A and B in the bulk and surface phase, respectively [5, 34].

The AlNi intermediate phase was postulated as energetically favored and the preferential interaction of Al and Ni atoms favor the formation of AlNi short-range order elements in the liquid phase. The presence of short-range order in the liquid phase increases the surface tension and its variations can be estimated by the difference between the surface tension isotherms calculated by the two models [5, 6]. The effects of the minority alloying elements on the

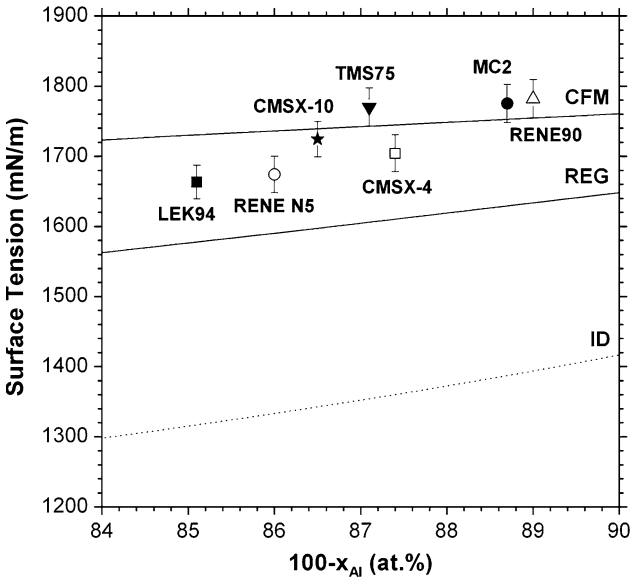

Fig. 9 Comparison between the surface tension experimental data of Ni-based superalloys (Table 4), and the calculated surface tension isotherms: CFM (compound formation model); REG (regular solution model); ID (ideal solution model). Experimental and theoretical data are calculated at $T = 1773$ K and reported as a function of Ni content in the alloy

surface tension of Ni-based alloys are comparable, at least to a first approximation, to that of liquid nickel itself. Therefore, for the calculation, the Ni content was taken as the sum of the amount of Ni present in the alloy plus the minority alloying elements. Accordingly, the surface tension values of the $Al_{11.3}Ni_{88.7}$, $Al_{12.9}Ni_{87.1}$, $Al_{13.5}Ni_{86.5}$, and $Al_{14.9}Ni_{85.1}$ alloys having the same Al content as the superalloys investigated represent the model systems for MC-2, CMSX-10, TMS-75, and LEK-94, respectively. The surface tension isotherms of Al–Ni liquid alloys were calculated using the three aforementioned models for 1773 K and together with new experimental data and literature data from our previous measurements of other Ni-based superalloys [12, 22] are shown in Fig. 9.

It is worth noting that the best agreement between the new experimental surface tension data and the model predicted values is obtained for the corresponding values calculated by the CFM, exhibiting a maximum difference of about 4.2 % (Table 4).

As clearly shown in Fig. 9, all the measured values are very close to those predicted by the CFM which accounts for short-range order phenomena: the surface tension of liquid superalloys is affected by the Al–Ni interactions between the nearest neighbor atoms which reduce the segregation of the surface active component to the surface.

The new surface tension datasets on MC-2, TMS-75, CMSX-10, and LEK-94 superalloys were further analyzed in the framework of thermodynamic models related to surface properties of ternary liquid alloys with the aim of evaluating the reliability of experimental data obtained. Chromium, with content of 9.30 at % is the third major component after Ni and Al in MC-2 (Table 1) and the surface tension of $Al_{11.3}Cr_{9.6}Ni_{79.1}$ ternary alloy having the same Al and Cr contents as the MC-2 was used for comparison (Fig. 10a).

Similarly, Ni, Al, and Co are the major components of TMS-75, CMSX-10, and LEK-94 superalloys, and their surface tension was compared to the corresponding values of $Al_{12.9}Co_{12.4}Ni_{74.7}$, $Al_{13.5}Co_{5.7}Ni_{80.8}$, and $Al_{14.9}Co_{7.5}Ni_{77.6}$, respectively (Fig. 10b). As mentioned previously, the contents of the minority alloying elements in Ni-based superalloys investigated were replaced by that of Ni.

The surface tensions of liquid Al–Cr–Ni and Al–Co–Ni alloys were calculated combining the corresponding descriptions of their binary subsystems using the Toop model [35].

The geometric models, including the Toop model have been originally developed to predict the thermodynamic properties of ternary systems and recently were also applied to calculate their thermophysical properties, such as the surface tension, viscosity, and molar volume [5, 36]. In particular, the Toop model is asymmetric one and it is

Table 4 Surface tension of Ni-based superalloys measured at $T = 1773$ K and the corresponding model-based predictions related to the Al–Ni binary system $\left(\hat{\sigma}^{100-Al}_{1773\ K}\right)$ and to the Al–Co–Ni or Al–Cr–Ni ternary systems $\left((\hat{\sigma})^{100-Al-Co(Cr)}_{1773\ K}\right)$

Alloy	x_{Al} (at %)	σ_{1773K} (mN m^{-1})	$\left(\hat{\sigma}^{100-Al}_{1773\ K}\right)$ (mN m^{-1})	$(\hat{\sigma})^{100-Al-Co(Cr)}_{1773\ K}$ (mN m^{-1})	Reference
RENE-90	7.5	1782	1785	1775	[12]
MC-2	11.3	1776	1765	1762	Present work
CMSX-4	12.0	1706	1760	1761	[22]
TMS-75	12.9	1770	1753	1750	Present work
CMSX-10	13.5	1725	1751	1750	Present work
RENE-N5	14.6	1675	1744	1740	[12]
LEK-94	14.9	1663	1742	1741	Present work

For comparison, the literature data on the superalloys previously measured under the same experimental conditions [12, 22] are also given

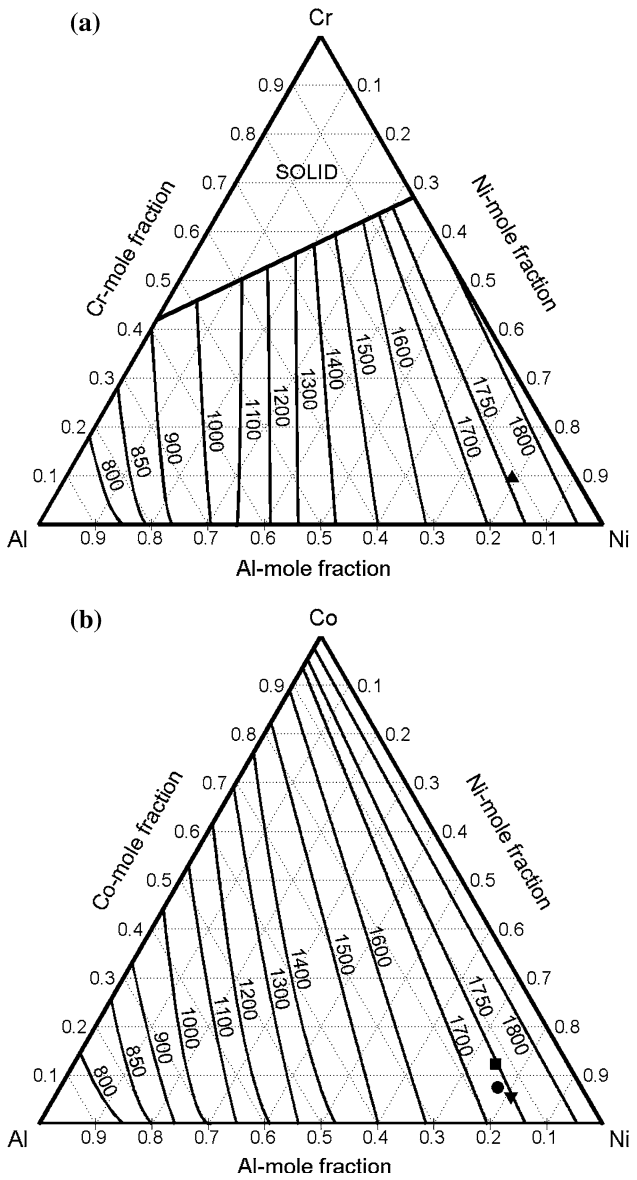

Fig. 10 Iso-surface tension lines calculated by the Toop geometric model for $T = 1773$ K. **a** liquid Al–Cr–Ni alloys; the symbol (*filled triangle*) indicates the $Al_{11.3}Cr_{9.6}Ni_{79.1}$ alloy used for the evaluation of validity and reliability of new surface tension data of MC-2 superalloy. **b** liquid Al–Co–Ni alloys; the $Al_{12.9}Co_{12.4}Ni_{74.7}$ (*filled square*), $Al_{13.5}Co_{5.7}Ni_{80.8}$ (*filled inverted triangle*), and $Al_{14.9}Co_{7.5}Ni_{77.6}$ (*filled circle*) alloys were used for the evaluation of validity and reliability of new surface tension data of TMS-75, CMSX-10, and LEK-94 superalloys, respectively

appropriate to describe the surface tension of the Al–Cr–Ni and Al–Co–Ni systems because two components of the both systems are similar to each other (in terms of the property under consideration) but differ markedly from the third component (Al). In the case of the Al–Co–Ni, the surface tension values of Al–Ni and Al–Co liquid alloys calculated by the CFM [5, 34] and those of Co–Ni alloys obtained by the QCA for regular solutions [32, 34] were combined into the Toop model. The same model was used to predict the surface tension of Al–Cr–Ni ternary alloys using as input the surface tensions of its binary subsystems calculated by the CFM [5, 33]. Full details of the mathematical formalism of the geometric models are reported in [5, 36]. The surface tension values of both ternary alloy systems calculated by the Toop model differ up 4.2 % from the new experimental values and all ternary values are slightly lower with respect to the Al–Ni values predicted by the CFM (Table 4). A comparison of measured and calculated values for the Ni-based superalloys analyzed is listed in Table 4, indicating that both model-based predictions substantiate fairly well the new surface tension experimental data and can be interpreted as a lower bound for the measured values in agreement with the findings reported by Mills et al. [21] related to uncertainty in the model-based predictions for different thermophysical properties of Ni-based superalloys. Indeed, in the case of surface tension, an uncertainty of about ±5 % was found.

Conclusion

The thermophysical properties of four commercial Ni-based alloys, namely MC-2, CMSX-10, TMS-75, and LEK-94, have been determined.

Calorimetric data on melting range, heat of fusion, specific heat, and fraction solid have been obtained from high-temperature thermal analysis. The heat of fusion compares well with that of a series of superalloys already known in the literature. The values of this quantity are all below the computed ideal enthalpy of melting indicating the occurrence of order in the liquid phase. The specific heat is close to that computed with the Neumann–Kopp rule. The fraction solid, determined here at various cooling rates, can be employed as an input information for simulating the solidification process by means of dedicated software.

Both density and surface tension have been measured in the liquid state in a wide temperature range, from the T_L, determined in this work, up to 1773 K. Measurements were performed under an atmosphere with very low oxygen contents and the accuracy of measurements was found to be < 3 and < 5 % for the surface tension and density, respectively. The results of both the properties have shown a linear dependence from the temperature in the entire temperature range. A dependence from the Al content in the alloy was observed: both surface tension and density decrease with the increasing of the Al content in the alloy.

In order to evaluate the reliability of the new experimental values, the obtained property datasets have been analyzed within various theoretical frameworks and compared with the literature data. Model-based predictions of

the surface tension and density of the two Ni-based superalloys exhibit a good agreement with the new experimental data.

The measured density values of superalloys investigated are consistent with each other and seem to confirm the hypothesis reported in the literature of a dependence on the γ' phase, i.e., Al content in the alloy.

Due to the reliability of the measurements performed in this work and inherent data scarcity, the new values of surface tension of the Ni-based superalloys, MC-2, CMSX-10, TMS-75, and LEK-94, are proposed as recommended data.

Acknowledgements This work was supported by the European Space Agency (ESA) Microgravity Applications Support Programme (MAP) under Contract No. 4200014306 (AO -99-022 and AO-2009-1020) and by the Italian Space Agency (ASI) under contract n. DC-MIC-2011-036. The authors wish to thank the ThermoProp Team for the fruitful discussions.

Compliance with ethical standards

Conflict of Interest The authors declare that they have no conflict of interest.

References

1. Furrer D, Fecht HJ (1999) Ni-based superalloys for turbine discs. JOM 51(1):14–17
2. Aune R, Battezzati L, Egry I, Etay J, Fecht HJ, Giuranno D, Novakovic R, Passerone A, Ricci E, Schmidt-Hohagen F, Seetharaman S, Wunderlich R (2005) Surface tension measurements of Al–Ni based alloys from ground-based and parabolic flight experiments: results from the thermolab project. Microgravity Sci Technol 18(3/4):73–76
3. Wunderlich R, Fecht HJ, Egry I, Etay J, Battezzati L, Ricci E, Matsushita T, Seetharaman S (2012) Thermophysical properties of a Fe–Cr–Mo alloy in the solid and liquid phase. Steel Res Int 83(1):43–54
4. Battezzati L, Baricco M, Pascale L (1998) High temperature thermal analysis of Ni–Al alloys around the γ' composition. Scr Mater 39:87–93
5. Egry I, Ricci E, Novakovic R, Ozawa S (2010) Surface tension of liquid metals and alloys—recent developments. Adv Colloid Interface Sci 159(2):198–212
6. Singh RN (1987) Short-range order and concentration fluctuations in binary molten alloys. Can J Phys 65:309–325
7. Sato A, Yeh AC, Kobayashi T, Yokokawa T, Harada H, Murakumo T, Zhang JX (2007) Fifth generation Ni based single crystal superalloys with superior elevated temperature properties. Energy Mater 2:19–25
8. Battezzati L, Baldissin D (2008) The Thermolab Project: thermophysical properties of superalloys. High Temp Mater Process 27:423–428
9. Ricci E, Arato E, Passerone A, Costa P (2005) Oxygen tensioactivity on liquid-metal drops. Adv Colloid Interface Sci 117(1–3):15–32
10. Maze C, Burnet G (1971) Modifications of a non-linear regression technique used to calculate surface tension from sessile drops. Surf Sci 24:335–342
11. Iida T, Guthrie RIL (1993) The physical properties of liquid metals, 1st edn. Clarendon Press, Oxford
12. Giuranno D, Amore S, Novakovic R, Ricci E (2015) Surface tension and density of RENE N5® and RENE 90® Ni—based superalloys. J Mater Sci 50:3763–3771. doi:10.1007/s10853-015-8941-0
13. Plevachuk Y, Egry I, Brillo J, Holland-Moritz D, Kaban I (2007) Density and atomic volume in liquid Al–Fe and Al–Ni binary alloys. Int J Mater Res 98(2):107–111
14. Ricci E, Amore S, Giuranno D, Novakovic R, Tuissi A, Sobczak S, Nowak R, Korpala B, Bruzda G (2014) Surface tension and density of Si-Ge melts. J Chem Phys 140:214704
15. Mukai K, Li Z, Mills KC (2005) Prediction of the densities of liquid Ni-based superalloys. Metall Mater Trans 36B:255–262
16. Li Z, Mills KC, McLean M, Mukai K (2005) Measurement of the density and surface tension of Ni-based superalloys in the liquid and mushy states. Metall Mater Trans 36B:247–254
17. Giuranno D, Tuissi A, Novakovic R, Ricci E (2010) Surface tension and density of Al–Ni alloys. J Chem Eng Data 55(9):3024–3028
18. Ansara I, Dupin N, Lukas HL, Sundman B (1997) Thermodynamic assessment of the Al–Ni system. J Alloys Compd 247:20–30
19. Mukai K, Li Z, Fang L (2004) Measurement of the densities of nickel-based ternary, quaternary and commercial alloys. Mater Trans 45(10):2987–2993
20. Quested PN, Brooks R, Chapman L, Morrell R, Youssef Y, Mills KC (2009) Measurement and estimation of thermophysical properties of nickel based superalloys. Mater Sci Technol 25(2):154–162
21. Mills KC, Youssef YM, Li Z, Su Y (2006) Calculation of thermophysical properties of Ni-based superalloys. ISIJ Int 46(5):623–632
22. Ricci E, Giuranno D, Novakovic R, Matsushita T, Seetharaman S, Brooks R, Chapman LA, Quested PN (2007) Density, surface tension, and viscosity of CMSX-4® superalloy. Int J Thermophys 28:1304–1321
23. Matsushita T, Fecht HJ, Wunderlich R, Egry I, Seetharaman S (2009) Studies of thermophysical properties of commercial CMSX4 alloy. J Chem Eng Data 54:2584–2592
24. Aune R, Battezzati L, Brooks R, Egry I, Fecht HJ, Garandet JP, Hayashi M, Mills KC, Passerone A, Quested PN, Ricci E, Schmidt-Hohagen F, Seetharaman S, Vinet B (2005) Thermophysical properties of IN738LC, MM247LC AND CMSX-4 in the liquid and high temperature solid phase. In: Loria EA (ed) International symposium on superalloys 718, 625, 706 and various derivatives, TMS, Warrendale
25. Nowak R, Lanata T, Sobczak N, Ricci E, Giuranno D, Novakovic R, Holland-Moritz D, Egry I (2010) Surface tension of c-TiAl-based alloys. J Mater Sci 45:1993–2001. doi:10.1007/s10853-009-4061-z
26. Dupin N, Ansara I, Sundman B (2001) Thermodynamic reassessment of the ternary system Al–Cr–Ni. Calphad 25(2):279–298
27. N. Dupin (1995) Contribution à l'évaluation thermodynamique des alliages polyconstitués à base de nickel, Lab. de Thermodynamique et de Physco-Chimie Métallurgiques de Grenoble
28. Lang G, Laty P, Joud JC, Desré P (1977) Measurement of the surface tension of some fluid metals by different methods. Z Metallkd 68:113–116
29. Naidich YuV, Perevertailo VM, Nevodnik GM (1972) Surface properties of Ni–C and Co–C melts. Izv Russ Akad Nauk Ser Metal 2:22–30
30. Levin ES, Ayushina GD (1971) Russ J Phys Chem 45(6):792–795
31. Lucas LD, Kozakevitch P (1971) Compte rendu du 12e séminaire de Thermodynamique et Physicochimie Métallurgiques ENSEEG-

IRSID publié par l'École Nationale Supérieure d'Électrochimie et d'Électrométallurgie de Grenoble
32. Novakovic R, Zivkovic D (2005) Thermodynamics and surface properties of liquid Ga-X (X = Sn, Zn) alloys. J Mater Sci 40:2251–2257. doi:10.1007/s10853-005-1942-7
33. Novakovic R (2011) Bulk and surface properties of liquid Al-Cr and Cr-Ni alloys. J Phys 23(1–8):235107
34. Novakovic R, Tanaka T (2006) Bulk and surface properties of Al-Co and Co-Ni liquid alloys. Physica B 371:223–231
35. Toop GW (1965) Predicting ternary activities using binary data. Trans Metall Soc AIME 233:850–855
36. Plevachuk Yu, Sklyarchuk V, Gerbeth G, Eckert S, Novakovic R (2011) Surface tension and density of liquid Bi-Pb, Bi-Sn and Bi-Pb-Sn eutectic alloys. Surf Sci 605(11–12):1034–1042